Materials Research Letters

ISSN: 2166-3831 (Online) Journal homepage: www.tandfonline.com/journals/tmrl20

Superplastic-like flow in a fine-grained equiatomic CoCrFeMnNi high-entropy alloy

S. R. Reddy, S. Bapari, P. P. Bhattacharjee & A. H. Chokshi

To cite this article: S. R. Reddy, S. Bapari, P. P. Bhattacharjee & A. H. Chokshi (2017) Superplastic-like flow in a fine-grained equiatomic CoCrFeMnNi high-entropy alloy, Materials Research Letters, 5:6, 408-414, DOI: 10.1080/21663831.2017.1305460

To link to this article: https://doi.org/10.1080/21663831.2017.1305460

© 2017 The Author(s). Published by Informa UK Limited, trading as Taylor & Francis Group.

Published online: 27 Mar 2017.

Submit your article to this journal

Article views: 5110

View related articles

View Crossmark data

Citing articles: 23 View citing articles

Full Terms & Conditions of access and use can be found at
https://www.tandfonline.com/action/journalInformation?journalCode=tmrl20

MATER. RES. LETT., 2017
VOL. 5, NO. 6, 408–414
https://doi.org/10.1080/21663831.2017.1305460

MATERIALS RESEARCH LETTERS
Taylor & Francis
Taylor & Francis Group

ORIGINAL REPORT

OPEN ACCESS
Check for updates

Superplastic-like flow in a fine-grained equiatomic CoCrFeMnNi high-entropy alloy

S. R. Reddy[a], S. Bapari[b], P. P. Bhattacharjee[a] and A. H. Chokshi[b]

[a]Department of Materials Science and Metallurgical Engineering, IIT Hyderabad, Hyderabad, India; [b]Department of Materials Engineering, India Institute of Science, Bengaluru, India

ABSTRACT

A CoCrFeMnNi high-entropy alloy (HEA) showed elongation to failure $\sim$320% at $T = 1023$ K and a strain rate $\dot{\varepsilon} = 10^{-4}\,\mathrm{s}^{-1}$. Strain hardening and texture weakening occurred at low $\dot{\varepsilon}$, whereas flow softening and texture strengthening were observed at high $\dot{\varepsilon}(> 3 \times 10^{-2}\,\mathrm{s}^{-1})$ experiments. The strain rate sensitivity (m) decreased from 0.5 to $\sim$0.25 with increasing $\dot{\varepsilon}$. Deformation with $m \sim 0.5$ and deformation-enhanced grain growth at low $\dot{\varepsilon}$ indicated superplasticity associated with grain boundary sliding. The grain boundary diffusion coefficient diminished by a factor of $\sim$4 in the HEA. Concurrent nucleation, growth and cavity interlinkage caused premature failure compared with conventional superplastic alloys.

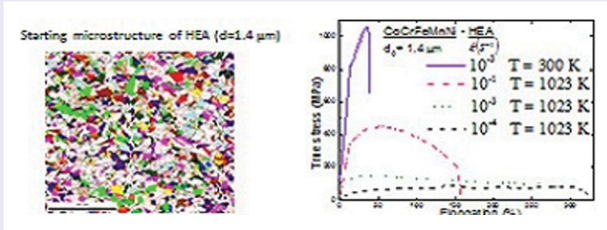

IMPACT STATEMENT

FCC CoCrFeMnNi HEA shows superplastic-like flow with $\sim$320% elongation at 1023 K and $10^{-4}\,\mathrm{s}^{-1}$ strain rate originating from grain boundary sliding.

ARTICLE HISTORY
Received 21 December 2016

KEYWORDS
High-entropy alloys; superplasticity; strain rate sensitivity; texture; cavitation

1. Introduction

High-entropy alloys (HEA), consisting typically of five or more elements, are a new class of alloys that have been developed over the past decade or so [1–6]. Many of these materials form concentrated solid solution alloys, and they have potentially interesting physical and mechanical properties. A recent review on HEA noted that there was very limited information available from tensile testing of such materials, especially at high temperatures [5].

The focus of this study is an equiatomic CoCrFeMnNi FCC alloy that has been widely investigated, and has become a standard material for scientific studies. Although early studies suggested that the material retained a single-phase structure upon extended exposure to high temperatures, more recent studies show that fine second-phase particles may develop in such materials depending upon the annealing conditions as well as the previous mechanical treatments [7–9]. Therefore, it is appropriate to consider the CoCrFeMnNi HEA as a quasi-single-phase alloy.

Mechanical testing data at high temperatures can be represented by an expression of the following form:

$$\dot{\varepsilon} \propto \sigma^n d^{-p} D, \tag{1}$$

where $\dot{\varepsilon}$ is the strain rate, σ is the stress, d is the grain size, D is the appropriate diffusion coefficient, and n and p are termed the stress exponent and inverse grain size exponent, respectively. Intragranular dislocation creep processes involve $n \gtrsim 3$ and $p = 0$, whereas superplasticity is usually associated with $n < 3$ and $p > 0$.

Tensile experiments on specimens with grain sizes of 155, 50 and 4.5 μm revealed that the tensile elongation to failure (e_f) decreases to $\sim$20% with increasing temperature up to 1073 K for the coarser grain sizes [10].

CONTACT P. P. Bhattacharjee pinakib@iith.ac.in Department of Materials Science and Metallurgical Engineering, IIT Hyderabad, Hyderabad, India; A. H. Chokshi achokshi@materials.iisc.ernet.in Department of Materials Engineering, India Institute of Science, Bengaluru 560 012, India

© 2017 The Author(s). Published by Informa UK Limited, trading as Taylor & Francis Group.
This is an Open Access article distributed under the terms of the Creative Commons Attribution License (http://creativecommons.org/licenses/by/4.0/), which permits unrestricted use, distribution, and reproduction in any medium, provided the original work is properly cited.

However, there was a slight increase in ductility with e_f of $\sim$50% in the 4.5 μm specimen at $T = 1073$ K [10]. Another investigation on specimens with a grain size of 12 μm and $T \sim 1023$–1123 K concluded that deformation occurred by a dislocation solute drag process with a stress exponent of $n \sim 3$, with a transition to $n \sim 5$ at higher strain rates [11].

An overview on HEA identified an elongation to failure of > 300% for superplasticity [12]. Superplastic flow is usually examined from constant strain rate testing, and analysis yields a strain rate sensitivity m $(= n^{-1})$. A high value of $m > 0.3$ (or $n < 3$) retards flow localization and promotes superplasticity [13]. Conventional superplastic alloy design is based on developing a reasonably stable grain size of < 10 μm, with either a microduplex structure or a quasi-single microstructure with particles pinning grain boundaries. Although there have already been reports of superplasticity in microduplex HEA [14,15], it is of interest to examine the possibility of superplasticity in a quasi-single-phase HEA with none or a very small quantity of isolated second-phase particles. Note that although superplasticity is not observed usually in pure metals because of rapid grain growth at high temperatures, there are reports of superplasticity in a fine-grained ytrria-stabilized tetragonal zirconia [16,17] which exhibits sluggish grain growth as well as nano-Ni which developed isolated second-phase particles during high-temperature testing [18,19]. Therefore, the hypothesis we would like to examine is that a fine-grained CoCrFeMnNi HEA may exhibit superplastic flow.

Several approaches have been developed to produce fine-grained HEA, including thermo-mechanical treatments [20,21], severe plastic deformation [8,22] and spark plasma sintering of nano sized powders [23], and these have led to grain sizes of less than $\sim$2 μm. The HEA exhibits only limited grain growth up to 1073 K, which has been attributed to sluggish diffusion and a distorted matrix because of the high solute content [20].

We show here elongations to failure of $\gtrsim$300% in a thermo-mechanically processed HEA having an initial grain size of 1.4 μm, with an optimum strain rate sensitivity of $\sim$0.5–0.6 and $T = 1023$ K, which corresponds to a homologous temperature of 0.64 based on a melting temperature of 1605 K [24]. Furthermore, testing at high strain rates leads to dynamic recrystallization, whereas superplastic flow at lower strain rates leads to deformation-enhanced grain coarsening.

2. Experimental

An equiatomic CoCrFeMnNi HEA was vacuum arc-melted from pure elements (with purity 99.9%) and cast into a bar with dimensions $10 \times 20 \times 40$ mm. Rectangular samples with dimensions $10 \times 20 \times 5$ mm, cut from the as-cast bar, were homogenized at 1373 K for 6 h to attain chemical homogeneity. In order to break down the cast structure, the homogenized samples were cold-rolled to 50% reduction in thickness using a laboratory scale rolling mill having roll diameters of 140 mm (SPX Precision Instruments, Fenn Division, USA). The rolled samples were annealed at 1073 K for 1 h and these samples were further warm rolled at 473 K to 85% reduction in thickness. Miniature tensile samples of gauge length 3 mm and width of 1 mm were electro-discharge machined (EDM) and further annealed at 973 K for 15 min to obtain a grain size of 1.4 μm. The tensile specimens had shoulders with a radius of curvature of 1 mm, connecting the gauge length to the grips; the nominal elongations reported include some limited deformation in the shoulder section. These samples were finely mechanically polished and then electropolished to remove any surface damaged zone. The final specimen thickness was typically $\sim$300 μm. The tensile loading direction was along the prior rolling direction (RD).

Uniaxial tensile tests were performed in air using a table top tensile machine (INSTRON 5567) and a three zone heating furnace (ATS, USA). Tensile testing was conducted primarily at 1023 K over strain rates from $\sim 10^{-4}$ to 10^{-1} s^{-1}. The tensile samples were heated from room temperature to 1023 K at 10 K min^{-1} and soaked for 20 min before starting the test; the samples were furnace cooled after the test. Strain rate cycling tests were conducted to evaluate the variation in strain rate sensitivity with strain rate and strain. The experiments reported here were conducted on electropolished specimens; experiments on specimens without polishing after EDM or after a substantially reduced thickness yielded somewhat lower ductility but similar flow stresses.

Selected samples were examined before and after failure to evaluate changes in the grain size and texture in the gripping region as well as a region near the fracture tip. The microstructural characterization involved an electron backscatter diffraction system (Oxford Instruments, UK) mounted on a scanning electron microscope (SEM) (Carl-Zeiss, Germany; Model: SUPRA 55). The grain size was determined from areal measurements.

3. Results

Figure 1 illustrates the variation in flow stress with nominal elongation for a specimen tested at room temperature and a strain rate of 10^{-3} s^{-1} and also tests at 1023 K and strain rates between 10^{-1} and 10^{-4} s^{-1}. While the room temperature test yielded a high maximum stress of $\sim$1050 MPa, the ductility was limited to an elongation to failure (e_f) of $\sim$35%. In contrast, the flow

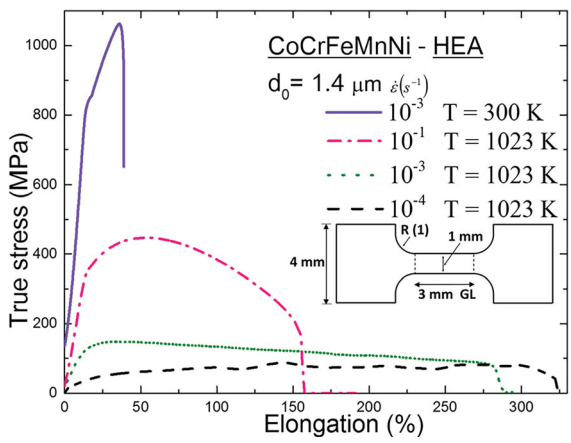

Figure 1. True stress–elongation (%) curve at 300 and 1023 K for different strain rates. The geometry of the tensile specimen is shown in the inset.

stresses were much lower at 1023 K, but the ductilities were much higher. Note the flow softening at $10^{-1}\,s^{-1}$ with e_f of $\sim$160%, and strain hardening at $10^{-4}\,s^{-1}$ and e_f of $\sim$320%. These results are similar to those reported in conventional microduplex superplastic metallic alloys [13], and also on a microduplex HEA [14,15].

The variation in strain rate sensitivity with strain rate and strain is depicted in Figure 2, from a plot of flow stress with nominal elongation at various strain rates. The strain rate sensitivities calculated from such data show a decrease in m from $\sim$0.59 at $10^{-4}\,s^{-1}$ to $\sim$0.25 at $10^{-2}\,s^{-1}$. Similar values of strain rate sensitivities were observed during the strain rate decrease cycle and the second strain rate increase cycle, although there seemed to be a slight decrease from m $\sim$0.6 to $\sim$0.5 at the lower strain rates. In terms of superplastic flow, the above behavior is consistent with a transition from a superplastic region II with high m at intermediate strain rates to a non-superplastic region III with low m at high strain rates [13].

Langdon [25] developed a unified model of superplasticity involving grain boundary sliding, which is consistent with data on a wide range of materials, and this leads to the following rate equation for superplastic flow $\dot{\varepsilon}_{sp}$

$$\dot{\varepsilon}_{sp} = \frac{AD_{gb}Gb}{kT}\left[\frac{b}{d}\right]^2\left[\frac{\sigma}{G}\right]^2, \qquad (2)$$

where the constant $A = 10$. D_{gb} is the grain boundary diffusion coefficient, b is the magnitude of the Burgers vector and G is the shear modulus. The experimental data in Figure 2 reveal a flow stress of 40 MPa at a strain rate of $10^{-4}\,s^{-1}$. Putting these values in Equation (2), along with $G = 56$ GPa [26], $b = 0.36$ nm [11], $d = 1.4\,\mu$m and $T = 1023$ yields a diffusion coefficient $D_{gb} = 2 \times 10^{-13}\,m^2\,s^{-1}$.

In an equiatomic HEA, the diffusion coefificent is likely to be controlled by the slowest moving species, which is Ni in the CoCrFeMnNi HEA. Prokoshkina et al. [27] studied grain boundary diffusion experimentally in Ni, and assuming a grain boundary width $\delta = 1$ nm their data yield a grain boundary diffusion coefficient of $8.7 \times 10^{-13}\,m^2\,s^{-1}$ at 1023 K. Thus, the current experimental observations are consistent with the widely accepted model for superplasticity, based on grain boundary sliding, in other classes of fine-grained materials. The calculations based on Equation (2) yield

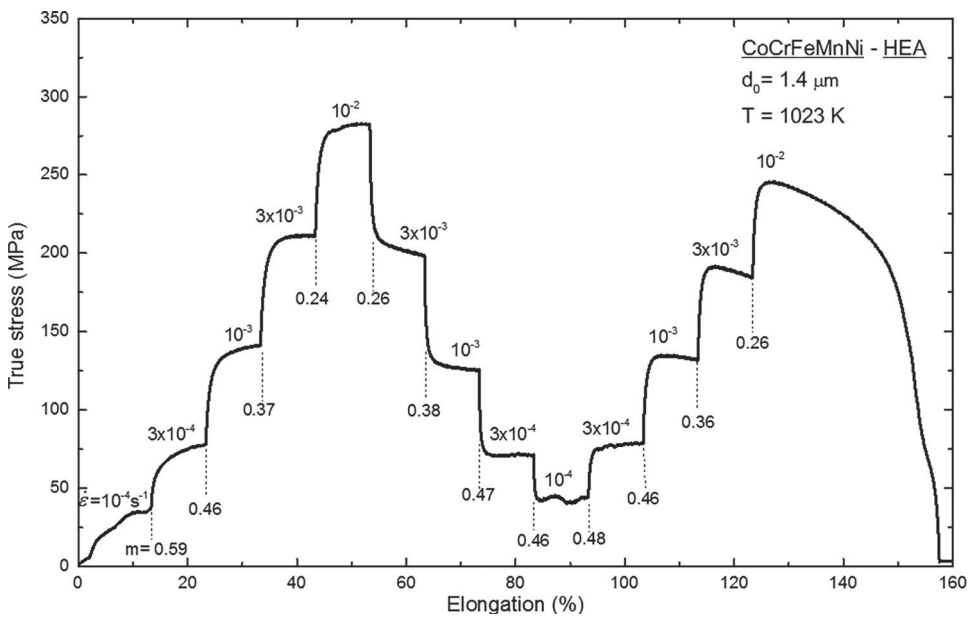

Figure 2. Stain rate jump test for different strain rates.

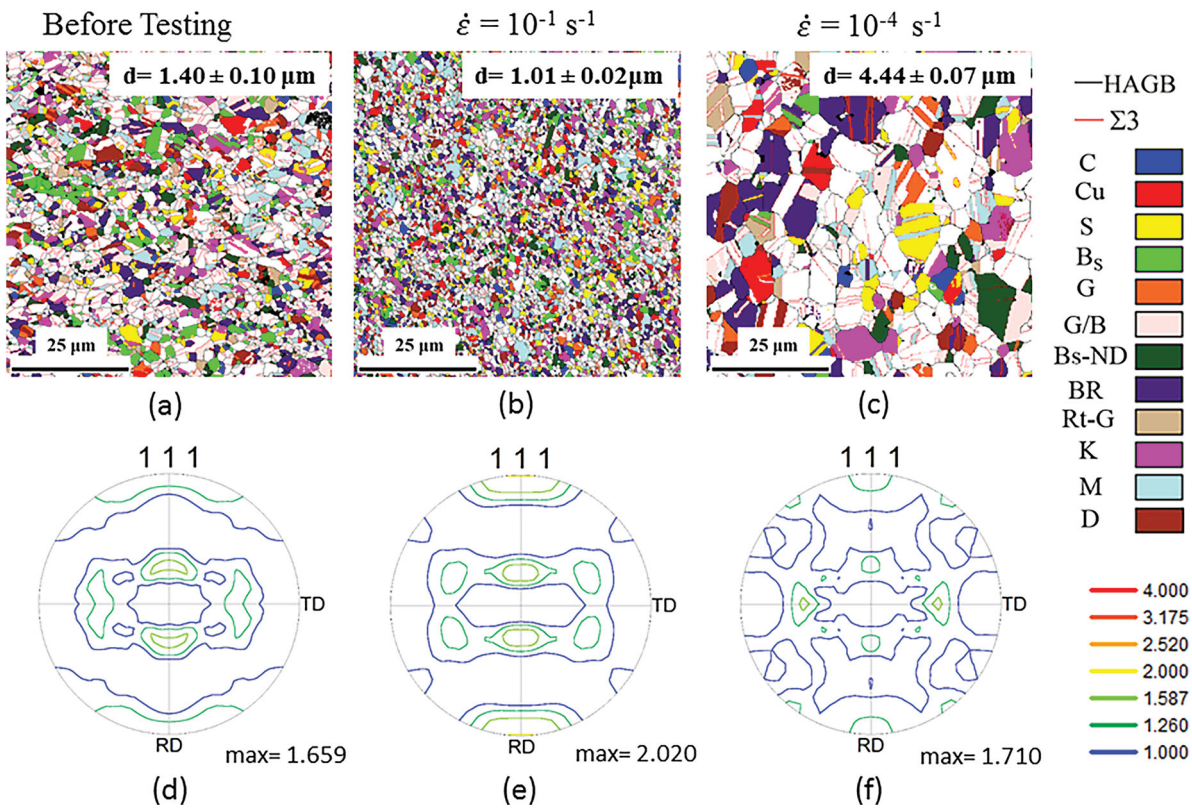

Figure 3. Orientation maps of deformed specimens at different strain rates and their corresponding (111) pole figures.

a diffusion coefficient that is about a factor of 4 lower than that for pure Ni; the slightly reduced diffusion coefficient may be consistent with the general observation of a decrease in diffusion coefficients in Ni with lower purity [27]. In addition, these results imply that while diffusion in HEAs may be sluggish at lower temperatures, it is not so at reasonably high temperatures as noted also from the observations of static grain growth at 1023 K from the grip sections of the specimens.

Microstructural information obtained in the study is summarized in Figure 3, where the upper and lower figures show the orientation maps and (111) pole figures, respectively, before testing and in regions near the fracture tips of specimens tested at 10^{-1} and 10^{-4} s^{-1}. There are three important points to note from these data. First, whereas high strain rate testing leads to a decrease in the grain size, low strain rate testing leads to an increase in the grain size. Second, there is noticeable increase in twins in the coarser grains at the lower strain rate. Third, while testing at 10^{-1} s^{-1} leads to a sharpening of texture consistent with intragranular dislocation activity, there is a weakening of texture at the lower strain rate that is expected when grain boundary sliding is significant.

It is important to distinguish the influence of time of exposure to elevated temperatures from deformation, in causing the above microstructural changes. Table 1 compares the grain sizes in the grip regions and near the fracture tips of specimens tested at 10^{-1} and 10^{-4} s^{-1}. In the absence of deformation, data from the grip regions reveal the occurrence of time-induced grain growth at 1023 K. However, the grain size is substantially reduced near the fracture tip of the sample tested at 10^{-1} s^{-1}, and the grain size is greater than the grip section of the sample tested at 10^{-4} s^{-1}. Taken together, the experimental results imply the occurrence of dynamic recrystallization at 10^{-1} s^{-1} and deformation-enhanced grain growth at 10^{-4} s^{-1}. Deformation-enhanced grain growth is a common observation in conventional superplastic materials [28], and it is usually associated with grain boundary sliding.

Table 1. Grain sizes in the grip sections and near fracture tips.

Strain rate (s^{-1})	Grip section (µm)	Near fracture (µm)
10^{-1}	1.80 ± 0.11	1.01 ± 0.02
10^{-4}	3.01 ± 0.08	4.44 ± 0.07

Since the present experiments were conducted at a constant cross-head velocity, the true strain rate decreases continuously as the specimen elongates. For a material exhibiting a high strain rate sensitivity, such a decrease in true strain rate is expected to lead to a decrease in flow stress at large strains. However, the

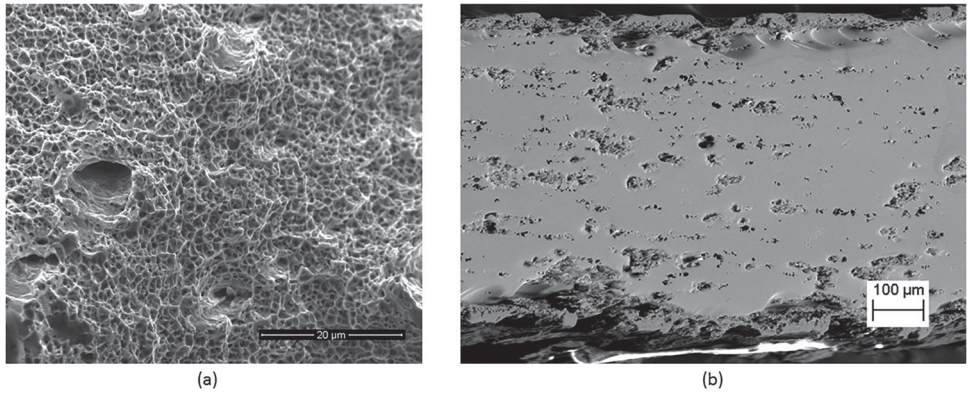

Figure 4. SEM image of (a) fracture tip of room temperature tensile test sample ($\dot{\varepsilon} = 10^{-3}\ s^{-1}$) and (b) polished sample of 1023 K tensile test sample ($\dot{\varepsilon} = 10^{-3}\ s^{-1}$).

data shown in Figure 1 indicate that there is no flow softening under superplastic flow conditions. The effective strain hardening observed in superplastic flow is likely to be a consequence of grain growth (as typically, $p > 0$) and/or the interference caused to the motion of intragranular dislocations by twins observed in the coarser grains. Models of superplasticity frequently consider the punching out of intragranular dislocations to relieve stress concentrations caused by grain boundary sliding at triple junctions [25], and there are experimental observations of intragranular dislocations being trapped in twin boundaries in a superplastic Cu alloy [29].

Figure 4 shows the fracture processes in specimens tested at room temperature (a) and under superplastic conditions at high temperature (b). The fracture surface shown in Figure 4(a) reveals a conventional ductile dimple fracture. Under superplastic conditions, a polished section of a fractured specimen reveals cavities in stringers aligned along the RD. The cavities were large, and the relatively broad cross-section near the fracture tip suggests that fracture occurred by the nucleation, growth and interlinkage of voids.

It is possible to analyze cavity nucleation in superplastic materials in terms of the stress concentrations induced by grain boundary sliding and local stress relaxations by diffusion [30]. However, it is difficult to apply such an analysis to the present HEA due to a lack of data on surface energies and grain boundary energies. The alignment of cavities in stringers may be a consequence of nucleation at particles introduced inadvertently during casting that are aligned along the RD, as observed in a quasi-single-phase superplastic Cu alloy [29], or may be associated with the superplastic deformation process, as noted in a microduplex Zn–22% Al eutectoid alloy [31]. It is interesting to note that cavity formation in stringers was also reported in superplastically deformed microduplex HEAs [14,15]. Although cavities appear to interlink in a direction parallel to the tensile axis, the high strain rate sensitivity limited cavity interlinkage perpendicular to the tensile axis, enabling superplastic flow. While a preliminary investigation suggested that fine particles had developed in the present HEA under high-temperature deformation, a more detailed investigation is necessary to identify the particles and their association with concurrent cavitation.

There are two additional issues that merit discussion: (a) the relatively low strain rate for superplasticity and (b) the relatively low elongation to failure.

In general, since the inverse grain size exponent p is typically in the range of 2–3, a decrease in grain size leads to increased strain rate (Equation (1)). Experiments on Al alloys have shown that when the grain size is reduced from ~ 10 to 1 µm, the optimum strain rate for superplasticity increases from $\sim 10^{-4}$ to $> 10^{-1}\ s^{-1}$. However, in the present HEA study the optimum superplasticity is a relatively low strain rate of $\sim 10^{-4}\ s^{-1}$ although the initial grain size was 1.4 µm. Inspection of Equation (1) reveals that the strain rate is also proportional to the diffusion coefficient, and it is likely that the enhancement in strain rate due to a finer grain size is offset by the somewhat lower diffusion coefficient in the HEA as well as significant concurrent grain growth. A further refinement in grain size to ultrafine or nanocrystalline regime may enable superplasticity at higher strain rates, although it may be difficult to retain a fine-grained structure in such quasi-single-phase HEA at high superplastic testing temperatures. Recent indentation experiments on HEA processed by high-pressure torsion to obtain a 40 nm grain size [22] suggest deformation by Coble creep ($n = m = 1$), which may yield superplasticity at room temperatures, if cracking or cavitation can be limited at the associated high stresses of ~ 0.5 to 1 GPa.

A strain rate sensitivity of ~ 0.5 gives large elongations to failure from $\gtrsim$500% in conventional superplastic

alloys. It is likely that concurrent cavitation during superplastic flow limited ductility in the present HEA. There is clearly a need to evaluate the cavity nucleation sites in the alloy. Ductility may also be limited by oxidation evident at surfaces of deformed samples and the limited number of grains across the thickness near the fracture tips. It is important to note that most commercial quasi-superplastic sheet forming operations require true strains < 1 [32], so that an elongation to failure of $> 300\%$ may be sufficient for the superplastic forming of the present HEA.

4. Conclusions

In summary, the present study demonstrated superplasticity in a fine-grained quasi-singe phase equiatomic CoCrFeMnNi alloy. Microstructural investigations revealed flow localization, dynamic recrystallization and texture sharpening at a high strain rate, with an elongation to failure of $\sim 160\%$, and more uniform flow with an elongation to failure of $\gtrsim 300\%$, deformation-enhanced grain growth and a weakening of texture at a low strain rate. The experimental data are consistent with a model for superplasticity based on grain boundary sliding. A further refinement in grain size and strategies for limiting grain growth may be useful approaches to enhancing ductility in such HEAs.

Acknowledgements

The authors sincerely acknowledge Professor J. W. Yeh of NTHU, Taiwan, for kindly providing the starting material used in this study.

Disclosure statement

No potential conflict of interest was reported by the authors.

Funding

SB and AHC acknowledge support of this work by the Department of Science and Technology (DST) at IISc Bangalore. SRR and PPB gratefully acknowledge the support of DST, India (Grant no. SB/S3/ME/47/2013).

References

[1] Yeh JW, Chen SK, Lin SJ, et al. Nanostructured high-entropy alloys with multiple principal elements: novel alloy design concepts and outcomes. Adv Eng Mater. 2004;6:299–303.
[2] Cantor B, Chang ITH, Knight P, et al. Microstructural development in equiatomic multicomponent alloys. Mater Sci Eng A. 2004;375–377:213–218.
[3] Zhang Y, Zuo TT, Tang Z, et al. Microstructures and properties of high-entropy alloys. Prog Mater Sci. 2014;61:1–93.
[4] Pickering EJ, Jones NG. High-entropy alloys: a critical assessment of their founding principles and future prospects. Int Mater Rev. 2016;61:183–202.
[5] Miracle DB, Senkov ON. A critical review of high entropy alloys and related concepts. Acta Mater. 2017;122:448–511.
[6] Murty BS, Yeh JW, Ranganathan S. *High-entropy alloys*. London, UK: Butterworth-Heinemann; 2014.
[7] Schuh B, Mendez-Martin F, Völker B, et al. Mechanical properties, microstructure and thermal stability of a nanocrystalline CoCrFeMnNi high-entropy alloy after severe plastic deformation. Acta Mater. 2015;96:258–268.
[8] Otto F, Dlouhý A, Pradeep KG, et al. Decomposition of the single-phase high-entropy alloy CrMnFeCoNi after prolonged anneals at intermediate temperatures. Acta Mater. 2016;112:40–52.
[9] Pickering EJ, Muñoz-Moreno R, Stone HJ, et al. Precipitation in the equiatomic high-entropy alloy CrMnFeCoNi. Scr Mater. 2016;113:106–109.
[10] Otto F, Dlouhý A, Somsen C, et al. The influences of temperature and microstructure on the tensile properties of a CoCrFeMnNi high-entropy alloy. Acta Mater. 2013;61:5743–5755.
[11] He JY, Zhu C, Zhou DQ, et al. Steady state flow of the FeCoNiCrMn high entropy alloy at elevated temperatures. Intermetallics. 2014;55:9–14.
[12] Lu ZP, Wang H, Chen MW, et al. An assessment on the future development of high-entropy alloys: summary from a recent workshop. Intermetallics. 2015;66:67–76.
[13] Chokshi AH, Mukherjee AK, Langdon TG. Superplasticity in advanced materials. Mater Sci Eng R. 1993;10:237–274.
[14] Kuznetsov AV, Shaysultanov DG, Stepanov ND, et al. Tensile properties of an AlCrCuNiFeCo high-entropy alloy in as-cast and wrought conditions. Mater Sci Eng A. 2012;533:107–118.
[15] Shaysultanov DG, Stepanov ND, Kuznetsov AV, et al. Phase composition and superplastic behavior of a wrought AlCoCrCuFeNi high-entropy alloy. J Miner. 2013;65:1815–1828.
[16] Wakai F, Sakaguchi S, Matsuno Y. Superplasticity of yttria-stabilized tetragonal ZrO_2 polycrystals. Adv Ceram Mater. 1986;1:259–263.
[17] Chokshi AH. Superplasticity in fine grained ceramics and ceramic composites: current understanding and future prospects. Mater Sci Eng A. 1993;166:119–133.
[18] Prasad MJNV, Chokshi AH. Superplasticity in electrodeposited nanocrystalline nickel. Acta Mater. 2010;58:5724–5736.
[19] Prasad MJNV, Chokshi AH. Microstructural stability and superplasticity in an electrodeposited nanocrystalline Ni–P alloy. Acta Mater. 2011;59:4055–4067.
[20] Bhattacharjee PP, Sathiaraj GD, Zaid M, et al. Microstructure and texture evolution during annealing of equiatomic CoCrFeMnNi high-entropy alloy. J Alloys Compd. 2014;587:544–552.
[21] Sathiaraj GD, Bhattacharjee PP, Tsai CW, et al. Effect of heavy cryo-rolling on the evolution of microstructure

and texture during annealing of equiatomic CoCrFeMnNi high entropy alloy. Intermetallics. 2016;69: 1–9.
[22] Lee DH, Seok MY, Zhao Y, et al. Spherical nanoindentation creep behavior of nanocrystalline and coarse-grained CoCrFeMnNi high-entropy alloys. Acta Mater. 2016;109: 314–322.
[23] Praveen S, Murty BS, Kottada RS. Phase evolution and densification behavior of nanocrystalline multicomponent high entropy alloys during spark plasma sintering. J Miner. 2013;65:1797–1804.
[24] Sathiaraj GD, Ahmed MZ, Bhattacharjee PP. Microstructure and texture of heavily cold-rolled and annealed FCC equiatomic medium to high entropy alloys. J Alloys Compd. 2016;664:109–119.
[25] Langdon TG. A unified approach to grain boundary sliding in creep and superplasticity. Acta Metall Mater. 1994;42:2437–2443.
[26] Laplanche G, Gadaud P, Horst O, et al. Temperature dependencies of the elastic moduli and thermal expansion coefficient of an equiatomic, single-phase CoCrFeMnNi high-entropy alloy. J Alloys Compd. 2015; 623:348–353.
[27] Prokoshkina D, Esin VA, Wilde G, et al. Grain boundary width, energy and self-diffusion in nickel: effect of material purity. Acta Mater. 2013;61:5188–5197.
[28] Chokshi AH. On the emergence of new surface grains during superplastic deformation. Scr Mater. 2001;44: 2611–2615.
[29] Falk LKL, Howell PR, Dunlop GL, et al. The role of matrix dislocations in the superplastic deformation of a copper alloy. Acta Metall. 1986;34:1203–1214.
[30] Chokshi AH. An experimental study on the alignment of cavities in a superplastic commercial copper alloy. Metall Trans A. 1987;18:63–67.
[31] Chokshi AH, Langdon TG. Cavitation and fracture in the superplastic Al-33% Cu eutectic alloy. J Mater Sci. 1989;24:143–153.
[32] Schroth JG. General motors' quick plastic forming process. Adv Superplasticity Superplastic Forming. 2004;9–20.